Nano Energy 30 (2016) 330–340

Contents lists available at ScienceDirect

Nano Energy

journal homepage: www.elsevier.com/locate/nanoen

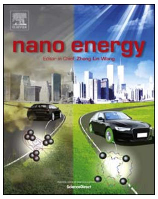

Structural engineering using rubidium iodide as a dopant under excess lead iodide conditions for high efficiency and stable perovskites

The Duong[a,*], Hemant Kumar Mulmudi[a], Heping Shen[a], YiLiang Wu[a], Chog Barugkin[a], Yahuitl Osorio Mayon[a], Hieu T. Nguyen[a], Daniel Macdonald[a], Jun Peng[a], Mark Lockrey[b], Wei Li[c], Yi-Bing Cheng[c], Thomas P. White[a], Klaus Weber[a], Kylie Catchpole[a,*]

[a] *Centre for Sustainable Energy Systems, Research School of Engineering, Australian National University, Canberra 2601, Australia*
[b] *Australian National Fabrication Facility, Research School of Physics and Engineering, Australian National University, Canberra 2601, Australia*
[c] *Department of Materials Science and Engineering, Monash University, Victoria 3800, Australia*

ARTICLE INFO

Keywords:
Perovskite solar cell
Rubidium
Cathodoluminescence
Photoluminescence
Lead excess
Stability

ABSTRACT

The highest efficiency perovskite solar cells reported so far are based on mixtures of formamidinium lead triiodide ($FAPbI_3$) and methylammonium lead tribromide ($MAPbBr_3$), where $MAPbBr_3$ acts as a stabilizer to improve the formation of the black perovskite phase. In this work, we dope the perovskite precursor mixture with rubidium iodide (RbI) and study the interplay between the doping substituent and the PbI_2 excess on the perovskite phase formation and film morphology. The addition of 5% RbI in combination with excess PbI_2 eliminates the formation of yellow non-perovskite phase and enhances the crystallinity of the films. However, the addition of more than 10% RbI results in the formation of a Rb-rich phase, which is detrimental for the cell performance. The findings are confirmed by cathodoluminescence measurements, which also reveal the spatial distribution of different phases on the perovskite films. The performance of RbI-doped perovskite cell is reported for the first time with the highest efficiency of 18.8% and improved thermal/photo stability compared to the undoped cells. The study demonstrates the potential of Rb as an alternative cation for use in high efficiency perovskite cells.

1. Introduction

Following the first reported efficiency of 3.8% in 2009, perovskite solar cells have emerged to reach a certified efficiency of 22.1% in 2016 [1–3]. With such high recorded efficiencies achieved by simple fabrication processes, perovskite solar cells are also very promising for complementing silicon solar cells in a tandem configuration. The organic-inorganic metal halide perovskite structure takes the form of ABX_3, where A is normally an organic mono-positive cation such as methylammonium (CH_3NH_3) (MA) or formamidinium ($HC(NH_2)_2$) (FA), B is a metal cation such as Pb, Sn and X is a halide anion such as I, Br, or Cl. The presence of the organic cation is one of the major concerns with the stability of perovskite solar cell under operational conditions. It has been reported that moisture, light, heat and electrical bias can all have a significant impact on the lifetime of the device [4]. In fact, a recent experimental study has suggested thermodynamic instability of $MAPbI_3$ due to it positive enthalpy (heats) of formation [5], emphasizing the need for finding more stable perovskite compositions. To address these issues, efforts to completely replace the organic cation by its inorganic equivalent caesium (Cs) have been reported with reasonable success [6–8]. $CsPbI_3$ has a bandgap of 1.7 eV, suitable for tandem solar cell applications as well as single junction solar cells, however it forms an orthorhombic structure at room temperature and transforms to cubic (perovskite) structure only at 634 K [9]. The high temperature required for the formation of the cubic phase of $CsPbI_3$ implies the structural instability of this material at room temperature. Efficiency of up to 8.4% for $CsPbI_3$ perovskite cells has been reported although the cell degrades rapidly (less than 1 h in ambient atmosphere) [10]. By partially replacing the larger iodide with the smaller bromide in the form of $CsPb(Br_xI_{1-x})_3$, improved structural phase stability has been observed with efficiency of 6.5%. Overall the efficiency achieved with the inorganic perovskite has been limited to less than 10%.

On the other hand, organic-inorganic perovskite with mixtures of $FAPbI_3$ and $MAPbBr_3$ (denoted as mixed perovskite) have emerged as suitable candidates to achieve superior efficiency [11]. $MAPbBr_3$ acts as a stabilizer to promote the formation of black α-$FAPbI_3$ phase. Following this strategy, high efficiencies have been achieved by using excess amount of

---

[*] Corresponding authors.
E-mail addresses: the.duong@anu.edu.au (T. Duong), kylie.catchpole@anu.edu.au (K. Catchpole).

http://dx.doi.org/10.1016/j.nanoen.2016.10.027
Received 9 August 2016; Received in revised form 12 September 2016; Accepted 14 October 2016

PbI_2 in the precursor, which significantly improves the open circuit voltage (V_{oc}) to as high as 1.18 V with an active material bandgap of 1.5–1.6 eV [12]. Another approach to have both high efficiency and stable perovskite solar cells is to combine the stability of inorganic mono-positive cations with the better efficiency achieved with organic cations. There are several reports investigating the effect of mixed-cation perovskite with Cs. One of the first reports by Lee et al. used the hybridization of Cs and FA ($FA_{0.9}Cs_{0.1}PbI_3$) to improve the photo- and moisture- stability of perovskite solar cells, which has been attributed to the enhanced FA-I interaction due to the contraction of the cubo-octahedral volume. The average efficiency improved from 14.9–16.5% due to Cs incorporation [13]. McMeekin et al. employed $FA_{0.83}Cs_{0.17}PbI_{1.8}Br_{1.2}$ to tune the optical bandgap to 1.75 eV for tandem applications. The compound was found to have better photo-stability than commonly used $MAPbI_{1-x}Br_x$ [14]. Following a similar approach, Yi et al. employed $Cs_{0.2}FA_{0.8}PbI_{2.84}Br_{0.16}$ to obtain an efficiency of up to 18% with excellent long term stability in ambient air (although the relative humidity is not specified in the report). The improvement comes from the entropic gain and the small internal energy input required for the formation of black perovskite phase upon the addition of Cs [15]. Li et al. demonstrated that the Goldschmidt's tolerance factor can be tuned to the optimal range by alloying $FAPbI_3$ and $CsPbI_3$, which result in better cell performance and stability [10]. Most recently Saliba et al. used a triple cation mixture consisting of MA/FA/Cs; efficiency of 21.1% was reported with better cell stability and process reproducibility. In that paper, the initial perovskite solution contains ~10% of excess PbI_2 which has been claimed to have a beneficial effect on the device performance although the PbI_2 peak is suppressed completely upon the addition of CsI as evident from the XRD measurement [16].

As suggested by above mentioned reports, the addition of a smaller size inorganic cation (such as Cs) leads to better performance and stability. This motivated us to investigate the effect of substituting Cs with rubidium (Rb) because of the even smaller size of Rb cation (1.52 Å) compared to Cs (1.81 Å). It is expected that due to the addition of Rb, the Goldschmidt tolerance factor will be in the vicinity of 1, hence enhancing the structural stability of the perovskite system. This might also have a positive impact on the thermal and moisture stability of the material. A previous study to understand the structural evolution of Cs and Rb triiodoplumbates found that both $CsPbI_3$ and $RbPbI_3$ crystallize in orthorhombic *Pnma* symmetry and expand isotropically upon heating. While $CsPbI_3$ undergoes a reversible phase transition to the cubic perovskite structure between the temperature range of 563–602 K, the $RbPbI_3$ does not undergo any phase transition until melting at high temperature of 700 K [9]. Ab initio calculation of bandgaps and absolute band position of polymorphs of $CsPbI_3$ and $RbPbI_3$ has shown that δ-$RbPbI_3$ has the electronic structure capable of efficient electron transfer to TiO_2 while δ-$CsPbI_3$ does not. Both of them, however, have low electron-hole mobility due to the flat band structure [17]. The above mentioned reports suggest that the alloying of organic cations perovskites with Rb could have a beneficial effect on their photovoltaic performance. However, to date there is no report investigating the functional photovoltaic performance of perovskite with Rb cation as a potential dopant. Our work reports the use of Rb for the first time in mixed-cation mixed-halide perovskite solar cells with improved device performance. Using both, cathodoluminescence (CL) and X-ray diffraction, we investigate the interplay of RbI with the excess PbI_2 on the formation of perovskite phases and film morphology. This study also demonstrates that Rb incorporation aids in enhancing the thermal- and photo-stability of perovskite solar cells.

2. Materials and methods

2.1. Materials

Poly[bis(4-phenyl)(2,5,6-trimentlyphenyl)amine (PTAA, M_n= 21,890 $gmol^{-1}$) was purchased from EM Index. Mesoporous transparent titania paste (30 NR-D), formamidinium iodide and methylammonium bromide were purchased from Dyesol and were used as received. All other materials were purchased from Sigma-Aldrich and were used as received unless specified otherwise.

2.2. Cell fabrication

FTO glass (TEC-7) was cleaned with detergent and ethanol in ultrasonic bath for 30 min and 10 min, respectively. A 30 nm-thick TiO_2 blocking layer (cp-TiO_2) was deposited on the clean glass using spray pyrolysis of a bis(isopropoxide)-bis(acetylacetonate)titanium(IV) solution at 450 °C. 200 nm-thick mesoporous TiO_2 (ms-TiO_2) was deposited on the substrate by spin-coating the solution of TiO_2 paste 30 NR-D in ethanol (1:6 of weight ratio) at 5500 rpm for 25 s with the acceleration rate of 1000 rpm/s. The sample was then annealed at 500 °C in air for 30 min. After cooling down to room temperature, the sample was immediately transferred to a N_2-filled glove box. Perovskite solution was prepared by mixing 1.1 M×(1+x) of PbI_2, 1.1 M FAI, 0.2 M $PbBr_2$, 0.2 M MABr in the mixture of DMF/DMSO (4:1 of volume ratio), where x is defined as the amount of excess PbI_2. 1.3 M of RbI solution in DMSO was added into the perovskite solution with varying amount for different doping concentration. Perovskite film was deposited on the sample with 2-step program consisting of 2000 rpm for 10 s and 6000 rpm for 20 s 10 s before the program ends, chlorobenzene was dropped on the spinning sample to accelerate the crystallization process [18]. The sample was then annealed at 100 °C for 30 min on a hotplate. 1 ml of PTAA solution was prepared by mixing the powder in toluene (10 mg/ml) with an additive of 7.5 μl (trifluoromethane)sulfonimide lithium salt (Li-TFSI) in acetonitrile (170 mg/ml) and 4 μl 4-*tert*-butylpyridine (TBP). The PTAA solution was spin-coated on the sample at 3000 rpm for 30 s with the acceleration rate of 3000 rpm/s. Finally 100 nm of Au contact was deposited on the sample through a shadow mask by thermal evaporation with the cell active area of 0.16 cm^2.

2.3. Characterization

X-ray diffraction was measured with a High-resolution PANalytical X'Pert PRO MRD system in Grazing Incidence X-ray Diffraction (GIXRD) with the step size of 0.005° and the integration time of 1 s per step. Reflection/Transmission was measured with Lambda 1050 spectrophotometer (Perkin Elmer) in the integrating sphere mode. The steady state photoluminescence spectra were captured using a Horiba Jobin Yvon Fluorolog FL3-22 system equipped with a 532-nm excitation diode-pumped solid state laser, and a photomultiplier tube (PMT) detector having a detection range from 400 to 1000 nm. The detail of the measurement setup can be found in the previous report [19]. The time-resolved photoluminescence was performed with a Horiba LabRAM Evolution system equipped with a 508-nm excitation pulsed laser, and another PMT detector having a detection range from 400 to 850 nm. All photoluminescence measurements were performed at room temperature and in air. Cathodoluminescence (CL) measurement was performed on FEI Verios scanning electron microscope (SEM) equipped with a Gatan MonoCL4 Elite cathodoluminescence system. Perovskite samples for CL measurements were prepared with a similar procedure to that described in the cell fabrication section. CL images were captured in panchromatic mode with appropriate dichroic filters. For imaging the perovskite-rich phase, a long pass filter (> 605 nm) was employed, while imaging of PbI_2 and Rb - rich phases was done using a band pass filter (505–575 nm). The CL imaging was performed at a constant accelerating voltage of 5 kV with a beam current of 13pA. Cross-sectional images were captured with Helios Nanolab 600 FIB system.

The external quantum efficiency (EQE) was measured using home-made setup without light bias in DC mode including a tungsten light source, a monochromators SP AB301-T, two Keithey 2425 source-meters, and a reference cell. The EQE response is calibrated using a